Molecular & Biochemical Parasitology 213 (2017) 1–11

Contents lists available at ScienceDirect

Molecular & Biochemical Parasitology

Evidence of the presence of a calmodulin-sensitive plasma membrane Ca^{2+}-ATPase in *Trypanosoma equiperdum*

María Carolina Pérez-Gordones[a], José Rubén Ramírez-Iglesias[b], Vincenza Cervino[a], Graciela L. Uzcanga[c], Gustavo Benaim[a,d], Marta Mendoza[b,*]

[a] *Instituto de Biología Experimental (IBE), Universidad Central de Venezuela (UCV), Caracas, Venezuela*
[b] *Centro de Estudios Biomédicos y Veterinarios, Instituto de Estudios Científicos y Tecnológicos (IDECYT), Universidad Nacional Experimental Simón Rodríguez (UNESR), Caracas, Venezuela*
[c] *Facultad de Ciencias Naturales y Ambientales, Universidad Internacional SEK (UISEK), Quito, Ecuador*
[d] *Instituto de Estudios Avanzados (IDEA), Caracas, Venezuela*

ARTICLE INFO

Article history:
Received 1 November 2016
Received in revised form 9 February 2017
Accepted 10 February 2017
Available online 14 February 2017

Keywords:
PMCA
Ca^{2+}-ATPase
Calmodulin
Animal trypanosomiasis
Trypanosoma equiperdum

ABSTRACT

Trypanosoma equiperdum belongs to the subgenus *Trypanozoon*, which has a significant socio-economic impact by limiting animal protein productivity worldwide. Proteins involved in the intracellular Ca^{2+} regulation are prospective chemotherapeutic targets since several drugs used in experimental treatment against trypanosomatids exert their action through the disruption of the parasite intracellular Ca^{2+} homeostasis. Therefore, the plasma membrane Ca^{2+}-ATPase (PMCA) is considered as a potential drug target. This is the first study revealing the presence of a PMCA in *T. equiperdum* (TePMCA) showing that it is calmodulin (CaM) sensitive, revealed by ATPase activity, western-blot analysis and immuno-absorption assays. The cloning sequence for TePMCA encodes a 1080 amino acid protein which contains domains conserved in all PMCAs so far studied. Molecular modeling predicted that the protein has 10 transmembrane and three cytoplasmic loops which include the ATP-binding site, the phosphorylation domain and Ca^{2+} translocation site. Like all PMCAs reported in other trypanosomatids, TePMCA lacks a classic CaM binding domain. Nevertheless, this enzyme presents in the C-terminal tail a region of 28 amino acids (TeC28), which most likely adopts a helical conformation within a 1–18 CaM binding motif. Molecular docking between *Trypanosoma cruzi* CaM (TcCaM) and TeC28 shows a significant similarity with the CaM-C28PMCA4b reference structure (2kne). TcCaM-TeC28 shows an anti-parallel interaction, the peptide wrapped by CaM and the anchor buried in the hydrophobic pocket, structural characteristic described for similar complexes. Our results allows to conclude that *T. equiperdum* possess a CaM-sensitive PMCA, which presents a non-canonical CaM binding domain that host a 1–18 motif.

1. Introduction

The Trypanosomatidae family encompasses a large number of unicellular organisms, many of which are causative agents of several tropical diseases that affect humans and animals. Livestock trypanosomoses caused by *Trypanosoma brucei brucei*, *Trypanosoma equiperdum* and *Trypanosoma evansi*, have a significant socio-economic impact and limit animal protein productivity throughout the world [1,2]. The identification and characterization of parasite proteins as chemotherapeutic targets is a current trend for the development of new parasitic disease treatments. It had been described that maintenance of Ca^{2+} homeostasis is vital for all organisms. Some drugs used in experimental treatment against trypanosomatids exert their action through the disruption of the parasite intracellular Ca^{2+} homeostasis [3]. High concentration of the ion usually results in cell death, while low intracellular concentrations are required for signal transduction and for the active sites of some enzymes [4,5].

The cytosolic Ca^{2+} concentration is maintained at a nanomolar range by various Ca^{2+} transport systems that are located in intracellular organelles and the plasma membrane of the cells [6]. One of

Abbreviations: PMCA, plasma membrane Ca^{2+}-ATPase; TePMCA, *Trypanosoma equiperdum* plasma membrane Ca^{2+}-ATPase; CaM, calmodulin; TcCaM, *Trypanosoma cruzi* calmodulin; TeC28, 28 amino acids region in the C-terminal of TePMCA; CaM-BD, calmodulin binding domain; CDMAP, Calmodulation Database and Meta-Analysis Predictor Server; TePMF, plasma membrane fraction from *T. equiperdum*; PDB id 2kne, the structure of Ca^{2+}-CaM in complex with C28 peptide from the binding domain of the PMCA isoform 4b.

* Corresponding author.
E-mail address: mendozamarta17@gmail.com (M. Mendoza).

http://dx.doi.org/10.1016/j.molbiopara.2017.02.001
0166-6851/

the major Ca^{2+} transporters is the plasma membrane Ca^{2+}-ATPase (PMCA). This pump belongs to the P-type ATPase family, and transports one Ca^{2+} to the extracellular space at the cost of the hydrolysis of one ATP molecule. PMCA has high Ca^{2+} affinity and is modulated by different agents. The major modulator of the enzyme is calmodulin (CaM), which induces a decrease of the Km for Ca^{2+} from 10–20 μM at the resting state to less than 1 μM following its interaction and also increases the Vmax of the enzyme [6–8].

Structurally, the pump presents 10 transmembrane domains, two large intracellular loops, and amino- and carboxy-terminal cytoplasmic tails [7]. Many PMCAs have a C-terminal, intracellular domain which autoinhibits the activity of the transporter, binding to "receptors" sites in the first and second cytoplasmic loops of the pump. The mechanism of CaM regulation of the PMCA involves the release of an autoinhibitory domain, which is removed upon binding of CaM to the C-terminal tail. In the presence of Ca^{2+}, CaM binds to this region at the CaM-binding domain (CaM-BD) and relieves the autoinhibition [6,9,10]. The CaM-BD at the C-terminal tail of PMCA4b is contained within a 28-residue peptide named C28 [11].

Many of the known Ca^{2+}/CaM binding proteins possess a region that is often characterized by a basic amphipathic helix consisting of approximately 20 amino acid residues. They contain positively charged amino acids interspersed among hydrophobic residues [12]. Several classes of CaM-binding motifs have been identified in these regions. In a classical manner, the Ca^{2+}/CaM binding motifs can be grouped into two major classes, designated as motifs 1–8-14 and 1–5-10, based on the position of conserved hydrophobic residues. The two lobes of CaM wrap around these motifs, enclosing it in a hydrophobic channel within the globular core [12,13]. Most recently, Juranic et al. [14] using solution NMR spectroscopy, obtained the structure of Ca^{2+}-CaM in complex with C28 peptide from the binding domain of the PMCA isoform 4b (PDB 2kne). The complex exhibits a new 1–18 CaM binding motif.

Similar to eukaryote cells, the PMCA is responsible for the regulation of the steady-state cytosolic Ca^{2+} concentration in trypanosomatids [15,16]. The pump in these parasites present similar characteristics to those described in higher eukaryotic systems [15,17–20]. PMCAs have been cloned in *T. cruzi* [19] and *T. brucei* [20]. Interestingly, at the molecular level, these PMCAs appear to lack a typical CaM-BD [21]. However, biochemical evidence for CaM stimulation has been reported in *T. cruzi* [17,22,23], *T. brucei* [15], *Leishmania braziliensis* [24], *Leishmania mexicana* [25], and *Leishmania donovani* [18]. Additionally, this enzyme can be isolated by a CaM-agarose column [17]. This might suggest that PMCAs of the trypanosomatid parasites contain a non canonical or different domain able to bind CaM.

Therefore, the aim of this work is to evaluate the presence of PMCA in *Trypanosoma equiperdum* and its modulation by CaM. *T. equiperdum* causes a disease called "dourine" or "covering sickness" in horses and other animals from the *Equidae* family and is spread primarily via sexual intercourse, an adaptation that has allowed it to escape beyond the range of the "tsetse fly' and attain a cosmopolitan distribution [26]. Differences in proteins involved in the Ca^{2+}-homeostasis can be used as potential targets for the development of novel therapeutic drugs to combat trypanosome infections. The general claim that PMCA could be a good drug target in a number of organisms is supported by significant phenotypic changes in organisms where the gene has been deleted or silenced [20,27,28].

2. Materials and methods

2.1. Parasite origin, maintenance and purification

The Venezuelan TeAp-N/D1 *Trypanosoma equiperdum* strain was initially isolated from the blood of a naturally infected horse from non determined locality of Apure State, Venezuela [29]. Blood samples prepared in phosphate-buffered saline (PBS), pH 8.0, containing 1% glucose and 10% DMSO were preserved in liquid nitrogen. Parasites were expanded in healthy male rats (Sprague–Dawley, 300 g body weight) by intraperitoneal injection (100 μl) of cryopreserved blood (~10^6 parasites/ml), and were purified from whole blood of infected animals by ionic exchange chromatography [30]. TeAp-N/D1 was previously considered as a *T. evansi* strain, termed TEVA1 [31–33]; however, recently has been classified as *T. equiperdum* by its molecular characterization using microsatellite markers and kinetoplast maxicircle genes [34].

2.2. Isolation of plasma membrane fraction of T. equiperdum

Plasma-membrane fraction of TeAp-N/D1 *T. equiperdum* strain (TePMF) was prepared essentially as reported previously [17,24]. Briefly, after a final wash in a medium containing 400 mM mannitol, 10 mM KCl, 2 mM EDTA, 1 mM phenylmethylsulphonyl fluoride (PMSF), 0.15 mg/ml soybean trypsin inhibitor, 10 μg/ml leupeptin and 20 mM Hepes-KOH, pH 7.4, the cell pellet was mixed with acid-washed glass beads (75–120 μM in diameter, Sigma) at a ratio of 1:4 (wet weight/weight of beads). The cells were disrupted by abrasion in a chilled mortar until 90% disruption was achieved as determined under an optical microscope. The glass beads, unbroken cells, and large debris were removed by centrifuging at 1000 g for 15 min at 4 °C. The supernatant was subjected to differential centrifugation, first at 16,000*g* for 30 min and then at 105,000*g* for 1 h, at 4 °C. The resulting pellet was resuspended in about 2 ml of medium containing 150 mM KCl, 50 μM $CaCl_2$, 2 mM $MgCl_2$, 10 μg/ml leupeptin, 1 mM PMSF, 0.15 mg/ml soybean trypsin inhibitor, 1 mM dithiothreitol (DTT), 5 μg/ml E64 and 75 mM Hepes-KOH, pH 7.2. The suspension was then gently passed three times through a Dounce homogenizer (AA; Arthur Thomas) immersed in an ice-cold water bath. Protein concentration was measured according to Lowry et al. [35], using bovine serum albumin (BSA) as a protein standard.

2.3. Determination of ATPase activity

Determination of ATPase activity was measured by a modification of the procedure described previously by Benaim et al. [22]. Briefly, aliquots of TePMF (about 0.5 mg of protein/ml) were incubated in a medium containing 75 mM Hepes-KOH, 150 mM KCl, 1 mM $MgCl_2$, 1 mM DTT, 1 mM ATP, 1 mM PMSF, 0.15 mg/ml soybean trypsin inhibitor, 10 μg/ml leupeptin, 5 μg/ml E64 pH 7.2 and the appropriate concentrations of $CaCl_2$ to obtain the desired free Ca^{2+} concentration. After 45 min incubation at 37° C, the reaction was arrested by the addition of 8% (final concentration) cold trichloroacetic acid. The mixture was centrifuged and the supernatant was kept for determination of Pi. The latter was carried out according to the method of Fiske and Subbarow [36], modified by the use of $FeSO_4$ as reducing agent. The Ca^{2+}-ATPase activity is expressed as the difference between the Mg^{2+}-ATPase activity in the presence of EGTA (without calcium) and the ATPase activity observed in the presence of Ca^{2+} and Mg^{2+}. Concentration of the ionic species and complexes at equilibrium were calculated by employing an iterative computer program modified from that described by Fabiato and Fabiato [37]. Ca^{2+}-ATPase activity was determined in the presence of various modulators and inhibitors of the enzyme for the characterization, such as: 10 μM calmidazolium (CMZ), 20 μM sodium orthovanadate, 1 μg/ml oligomycin and 8 μg/ml CaM (both commercial bovine brain and *T. cruzi*). *T. cruzi* CaM (TcCaM) was obtained by the protocol described previously by Garcia-Marchan et al. [38].

2.4. Western-blot analyses

Aliquots from TePMF and human erythrocyte purified PMCA (HsPMCA), containing 30 μg and 5 μg of total protein were resolved by SDS-PAGE [39] and electrotransferred to nitrocellulose membranes according to the procedure described by Towbin et al. [40]. The membrane was blocked by incubation with 1% gelatin in TBS (20 mM Tris-HCl pH 7.5, 0.5 M NaCl) for 1 h. The strips were incubated with commercial specific mouse monoclonal IgG antibody, produced against human PMCA (5F10 and JA3, raised against epitopes mapping amino acids 719–738 and 1135–1205 of PMCA4b respectively, Santa Cruz Biotechnology) or with specific polyclonal antibodies produced in rabbit against human PMCA purified from erythrocyte (diluted 1:200) [25]. Afterwards, the strips were incubated with horseradish peroxidase or alkaline phosphatase-conjugated secondary antibodies against rabbit or mouse IgG (diluted 1:10,000). Finally, protein band was visualized by the addition of diaminobenzidine (DAB) and hydrogen peroxide when horseradish peroxidase-conjugated antibodies were used, or nitroblue tetrazolium (NBT) and 5-bromo-4-chloro-3-indolyl phosphate (BCIP) when alkaline phosphatase-conjugated antibodies were employed. Human erythrocyte purified PMCA were used as positive control for the immunodetection.

2.5. Immuno-absorption

Inmuno-absortion was realized by a modification of the methodology described previously by Kurien [41]. Previously The 5F10 antibody (100 μl) diluted 1/20 in PBS (95 mM Na_2HPO_4, 5 mM NaH_2PO_4, pH 7.5, 150 mM NaCl) was dotted directly onto a nitrocellulose membrane and left dried for 1 h. Next, the membrane was blocked with 5% BSA in PBS for 1 h. Then, immuno-absorption of the corresponding antigens present in the TePMF carried out overnight at 4 °C. Membranes were washed 3 times with PBS by gently stirring over 15 min, between each step. Immune adsorbed proteins were extracted by incubation with 100 mM glycine pH 2.0, for 20 min. Subsequently, the solution was titled to pH 7.4 with Tris-base concentrate. Glycine was removed and the proteins were concentrated by centrifugation at 2500*g* using centricon (10,000 NMWL Millipore™). The protein analysis was performed by gel electrophoresis on 10% polyacrylamide SDS-PAGE as described above and visualized by silver staining.

2.6. Detection of CaM-binding proteins in the membrane fraction *from* T. equiperdum

Following SDS-PAGE, the TePMF was electron-transferred to nitrocellulose membranes as described above. The nitrocellulose sheet was blocked with 5% BSA in TBS (25 mM Tris-HCL pH 8.8, 150 mM NaCl, 2.7 mM KCl) containing 0.1% Tween-20. Specific CaM-binding proteins were visualized based on the protocol previously described by Billingsley et al. [42]. Briefly, the blots were incubated with 0.9 mg/ml of CaM-biotinylated (diluted 1/2000) and followed by detection with streptavidin conjugated to peroxidase (diluted 1:3000). Dilutions were carried out in TBS with or without calcium (0.2 mM $CaCl_2$ or 1 mM EGTA). All Incubations were made at room temperature for 1 h with agitation. The strips were washing 3 times for 15 min with TBS containing 0.1% Tween-20 between each step. For detection, the enhanced chemiluminescence method (ECL detection kit) was used following the instructions of the manufacturer (Amersham Life Science). Light emission from assays was recorded on an x-ray film with exposure time of 2 min.

Table 1
Primers designed from plasma membrane-type Ca2+-ATPases of *T. brucei* (TbPMC2).

Name	Nucleotide Sequence	Position
CD1	F: AAATTGTTGTGGGTGA R: TCACCCACAACAATTT	557–572
CD2	F:GTAGTGATAAAACTGGGACGCTGAC R:GTCAGCGTCCCAGTTTTATCACTAC	1145–1170
CD3	F:CTGTGACTGGTGATGGGACAAATGA R: TCATTTGTCCCATCACCAGTCACAG	2156–2180
CD4	F: TACAGCTGTTATGGGTAAATC R: AGATTTACCCATAACAGCTGTA	2436–2457
PMCA1	F: CATAAGACACAAGTATCAC	28–47
PMCA2	R: CCACATTACCTGGTAAAA	1333–1351
PMCA3	R: CATACACAAGGTTGCGGAAGTCC	2000–2023
PMCA4	F: CTTGGCATGTGCAACCGATACT	1627–1649
PMCA5	R: ACTTGAAACGCAATGCACGAACC	2799–2822
PMCA6	R: ACCATCCTTAATGTGTCA	3221–3239

CD: Conserved domain.
CD1: Cytosolic domain between II and III transmembrane regions, sequence EIVVGD.
CD2: Phosphorylation domain, sequence CSDKTGTLT.
CD3: ATP Binding domain, sequence AVTGDGTND.
CD4: C-terminal cytoplasmic domain, sequence VQLLWVNL.
PMCA1-6: specific sequences of plasma membrane-type Ca2+-ATPases of *T. brucei* (TbPMC2).

2.7. Purification of PMCA *from* T. equiperdum *by affinity-chromatographic with CaM-sepharose*

Purification of PMCA from TeAp-N/D1 *T. equiperdum* strain (TePMCA) was achieved by a modification of the procedure previously described by Benaim et al. [17]. Briefly, PMF was suspended at 3 mg/ml in a buffer containing 130 mM KCl, 50 μM $CaCl_2$, 0.5 mM $MgCl_2$ and 10 mM Hepes-KOH pH 7.2, were solubilized on ice for 10 min by adding Triton X-100 to a final concentration of 0.5% (w/v). The non-solubilized material was removed by centrifugation at 105,000*g* at 4 °C for 35 min. Phosphatidylcholine was then added to the supernatant to a final concentration of 0.5 mg/ml and the mixture was applied to a calmodulin-agarose column (3–4 ml bed volume), which was equilibrated in a buffer containing 0.4% (w/v) Triton X-100, 130 mM KCl, 20 mM Hepes-KOH pH 7.4, 1 mM $MgCl_2$, 100 μM $CaCl_2$, 2 mM DTT and 0.5 mg/ml of phosphatidylcholine. The column was then washed with the similar equilibration buffer containing 0.05% (w/v) Triton X-100. Finally, the PMCA was eluted in a buffer containing 0.05% (w/v) Tritón X-100, 130 mM KCl, 20 mM Hepes-KOH pH 7.4, 1 mM $MgCl_2$, 2 mM sodium EDTA, 2 mM DTT, 5% glycerol and 0.5 mg/ml of phosphatidylcholine. The Ca^{2+}-ATPase activity of the fractions eluted from the column was determined using the coupled enzyme system described previously by Benaim et al. [9]. After, fractions with activity were pooled. EDTA into pool fraction was chelated by the addition of 2 mM $MgCl_2$ at final concentration. Additionally, $CaCl_2$ was added to a final concentration of 50 μM. The purified ATPase was stored under N_2 at −70 °C.

2.8. PCR cloning and sequencing of the PMCA *from* T. equiperdum

Genomic DNA from purified *T. equiperdum* parasites was extracted using the Wizard Genomic DNA Purification Kit (Promega). DNA concentration (ng/μL) was estimated using a Nano Drop TM 1000 Spectrophotometer at 260 nm. To amplify the PMCA-like Ca^{2+}-ATPase gene, PCR was performed for 35 cycles at 94 °C for 30 s, 50–60 °C for 30 s, and 72 °C for 1 min, using a master mix (2X, Promega) with 10 ng of *T. equiperdum* genomic DNA, and 10 nM of each oligonucleotide primer corresponded to conserved domains (DC1-4 see Table 1) and specific domains (PMCA1-6 see Table 1) for a final volume of 25 μl. Oligonucleotide primers were design based on the *T. brucei* PMCA-like Ca^{2+}-ATPase sequence (*TbPMC2*, accession number Tb 927.08.1200. GenDB vacuolar type Ca^{2+}-ATPase, GI:

30315295) [20]. The obtained PCR products were cloned into PCR XL TOPO® vector (Life Technologies), analyzed by electrophoresis, purified (PCR purification kit, Promega), and sequenced in an ABI3130 sequencer (Applied Biosystems) by the dideoxynucleotide chain termination method [43] using the primers described.

2.9. Sequence analyses

The Biolign software (http://en.bio-soft.net/dna/BioLign.html) was used to assemble the *TeAp-N/D1 T. equiperdum* PMCA-like Ca^{2+}-ATPase gene (*TePMCA*) with the sequences obtained from the PCR products, and to translate the nucleotide sequence into amino acids. Similarity with other PMCA proteins was obtained by using BLAST (NCBI database). The ClustalW-PBIL program [44] from the European Bioinformatics Institute (EBI) was used to align the sequences of *TeAp-N/D1 T. equiperdum* PMCA-like Ca^{2+}-ATPase (TePMCA) and PMCA from *Homo sapiens* (PMCA4b, GI: 48255957) [46]. Classical and conserved domains of the P-type Ca^{2+}-ATPases were identified by the Inter-Pro Scan program from EBI. Additionally, other programs: TopPred [47], HMMTOP [48] and TMHMM (http://www.cbs.dtu.dk/services/TMHMM), were used to predict transmembrane helices and to perform a topology analysis of TePMCA. Analysis of the C-terminal sequence of the protein with the Calmodulation Database and Meta-Analysis Predictor (CDMAP) server (http://cam.umassmed.edu) [49], was performed to search the putative CaM-binding motifs within the TePMCA.

2.10. Molecular modeling and structural analyses

The homology model of TePMCA was established using the crystal structure of SERCA1 from *Oryctolagus cuniculus* as template (C3b9bA, conformation E2, 2.4 Å resolution) [50], and the C-terminal TePMCA homology model was established using the B chain corresponding to C28 of PMCA4b in the 2kne structure [14]. An initial model was obtained with the Phyre2 web portal for protein modeling, prediction, and analysis [51]. Validation of the generated model was carried out with PROCHECK programs [52] (https://prosa.services.came.sbg.ac.at/prosa.php & http://swift.cmbi.ru.nl/servers/html/index.html). Molecular figures were prepared using Discovery Studio 3.0 (Accelrys Software Inc). The TcCaM structure was modeled using as template the A chain from 2kne [14], in the Swiss–Model server (https://swissmodel.expasy.org) This model together with the putative CaM-BD sequence from TePMCA (TeC28, residues 1032–1059) were submitted to the CABS-Dock docking server (http://biocomp.chem.uw.edu.pl/CABSdock) [53]. A total of 200 simulations were used, suggesting an α-helix secondary structure for the ligand, with the rest of settings established as default. This server provides the coordinates of the docked structure and the contact maps of protein–protein interface. The docking obtained was superimposed with the 2kne structure (*Homo sapiens* CaM—C28 PMCA4b) [14], in order to calculate the ligand-RMSD. The TeC28 peptide and the TcCaM were separated and docked again using Hex 8.0 program [54] to calculate the energy score of the structure.

2.11. Statistical analysisd

All measurements were performed in triplicate with at least six biological replicates for each condition evaluated. The results of the Ca^{2+}- ATPase activity were expressed as the mean ± standard deviation (X ± SD) and compared with each experimental condition using the Student's *t*-test. Differences were considered to be statistically significant at values of $P < 0.05$.

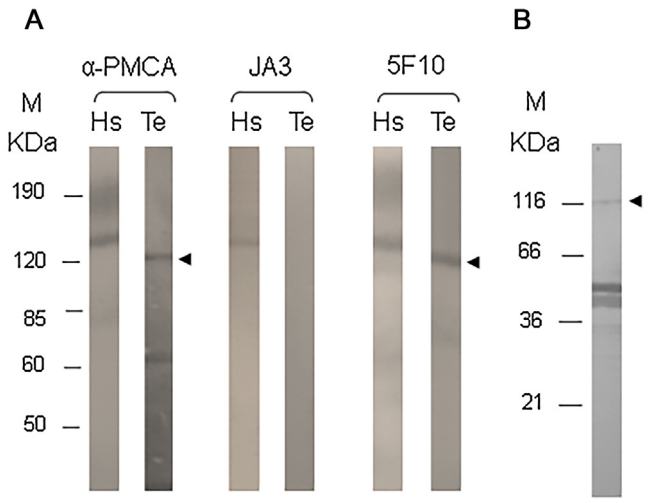

Fig. 1. Immunological evidence of the presence of PMCA in *T. equiperdum*. A) Immuno-staining of PMCA. Western-blot analysis of the binding of specific anti-(human purified erythrocyte PMCA) polyclonal antibody and the commercial specific anti-(human PMCA) monoclonal antibodies (5F10 and JA3) to human erythrocyte PMCA purified (Hs strip) and to plasma-membrane fraction from *T. equiperdum* (Te strip). B) Inmuno-absorption of *T. equiperdum* PMCA with the 5F10 antibody . Silver-stained SDS-PAGE of partially purified *T. equiperdum* PMCA. M: molecular weight marker. Arrow indicates the 120 molecular mass bands corresponding to *T. equiperdum* PMCA.

3. Results and discussion

Similar to vertebrates, a plasma membrane Ca^{2+}-ATPase (PMCA) is responsible for the regulation of the steady-state cytosolic Ca^{2+} concentration in trypanosomatids [21]. Although there are many studies related to Ca^{2+} regulation in trypanosomatids, as mentioned previously, there is an apparent controversy about the regulation of this enzyme by CaM in the literature. Even though some studies describe biochemical evidence for CaM stimulation, at the molecular level these PMCAs lack a typical CaM binding domain, as reported for mammalian PMCAs [21]. This study is the first to identify a PMCA in *T. equiperdum* (TePMCA) and presents strong evidence that support the presence of a CaM binding domain in these proteins.

3.1. Immunological evidences of the presences of PMCA in T. equiperdum

The presence of a TePMCA was supported by the recognition of a protein in the TePMF by α-PMCA specific antibodies. Thus, Fig. 1A shows the immunological cross-reactivity of the specific monoclonal antibody 5F10 against a protein of 120 kDa in the TePMF, whose molecular mass corresponds to that expected by the TePMCA (see below). The 5F10 epitope is highly conserved in most PMCAs from different origins and has been widely used for the identification of different isoforms of PMCA1/4 in higher eukaryotes [55]. Additionally, when a polyclonal antibody, generated against purified human erythrocyte PMCA, was used, it recognized the same band (Fig. 1A). Similarly, a 140 kDa protein was identified as the PMCA from *T. cruzi* using these specific antibodies [17]. Nevertheless, the antibody JA3 did not recognize any band in the TePMF. Instead, all the antibodies employed (α-PMCA, 5F10 and JA3) recognized a band of 140 kDA, which corresponds to the purified human red-blood cell Ca^{2+}-ATPase. Furthermore, both the polyclonal and monoclonal antibodies cross react with other minor band. The presence of additional bands has been observed by other authors with different cell preparations and antibodies against the plasma membrane Ca^{2+} pump [17,55]. These bands appear to be derived from

the 140 kDa band by proteolysis and/or aggregation, and their presence has been discussed previously [17,55]. No background staining was observed when the secondary antibodies were used as a control (results not shown).

Even more, the presence of a TePMCA was further supported in the present work by the immuno-absorption assays, where a partially purified enzyme was obtained. Thus, from the enriched TePMF the antibody 5F10 was able to precipitate the corresponding antigens, whose molecular mass is about 120 kDa, similar to that identified by immunostaining (Fig. 1B). Figure also shows other proteins of lower molecular mass, which may be derived by proteolysis from the 140 kDa band. Also, two intense bands of lower molecular mass were observed, which correspond to immunoglobulins (heavy and light chain). The recognition and precipitation by specific antibodies directed against PMCA corroborate the present of TePMCA.

3.2. Evaluation and characterization of PMCA activity in the plasma membrane fraction of T. equiperdum

Furthermore, the presence of TePMCA was demonstrated by the use of a highly enriched PMF from *T. equiperdum,* where we determined a Ca^{2+}-ATPase activity with similar characteristics to its counterpart in higher eukaryotes. Ca^{2+}-ATPase activity is operationally defined as the activity observed over the Mg^{2+}-ATPase when Ca^{2+} ions are added to the assay medium. TePMF hydrolyzed an appreciable amount of ATP in the absence of Ca^{2+} (44.16 ± 3.8 nmoles nmol Pi/min per mg of protein). Upon addition of micromolar amounts of Ca^{2+} in the presence of saturating Mg^{2+} concentrations additional ATPase activity, corresponding to a Ca^{2+}-ATPase was observed (Fig. 2A). As can be observed in Fig. 1A, the Ca^{2+} affinity of this ATPase became saturated with micromolar amounts of Ca^{2+}, reaching a *V*max of 8.2 ± 0.72 nmol Pi/min per mg of protein. The Km_{app} for Ca^{2+} was about 0.35 ± 0.03 μM in the absence of CaM. The TePMCA Ca^{2+} affinity was very high and comparable to those previously described for other PMCAs in trypanosomes [15,17,22,24,25]. Moreover, we demonstrated that TePMCA was CaM-sensitive, as described for different trypanosomatids [3]. The Ca^{2+}-ATPase activity was stimulated by CaM, resulting in a decreased of Km_{app} to 0.18 ± 0.05 μM, and a *V*max increased nearly 60% (13.24 ± 0.61 nmol Pi/min per mg of protein) when bovine CaM (8 μg/ml) was present in the medium Interestingly, when *T. cruzi* CaM instead of bovine CaM was present a larger stimulation was observed. Thus, the *V*max was increased up to 15.47 ± 0.59 nmol Pi/min per mg protein (increasing about 90%), while the Km_{app} (0.17 ± 0.06 μM) did not change significantly when compared to that obtained with bovine CaM (Fig. 2A and B). Albeit CaM is a highly conserved protein across the evolutionary scale, the stimulation of the Ca^{2+}-ATPase activity obtained with TcCaM was higher when compared to that obtained using CaM bovine. Interestingly, significant differences exist between *T. cruzi* and vertebrate CaM, such as 15 amino acid substitutions in its primary structure and a large increase in α-helix content upon binding with Ca^{2+} [38]. These differences could affect the CaM-enzyme interactions, being more efficient in the case of homologous proteins [18,38]. Even more, CaM stimulation was completely inhibited by the well known anti-CaM agent calmidazolium. As shown in Fig. 2B, the CaM antagonist (CMZ, 10 μM) inhibited the *T. cruzi* CaM stimulation (8.63 ± 0.58 nmol Pi/min per mg protein, $P > 0.05$). However, CMZ partially inhibited also the basal activity (7.26 ± 0.55 nmol Pi/min per mg protein, $P < 0.05$), but only 14% at the concentration used (Fig. 2B), thus indicating non-specific effects over the enzyme similar to those reported previously [22,56].

Similar to other 'P-type' pumps, low concentration of the classical ATPase inhibitor vanadate also strongly inhibits the TePMCA activity, indicating the formation of a phosphorylated intermediate

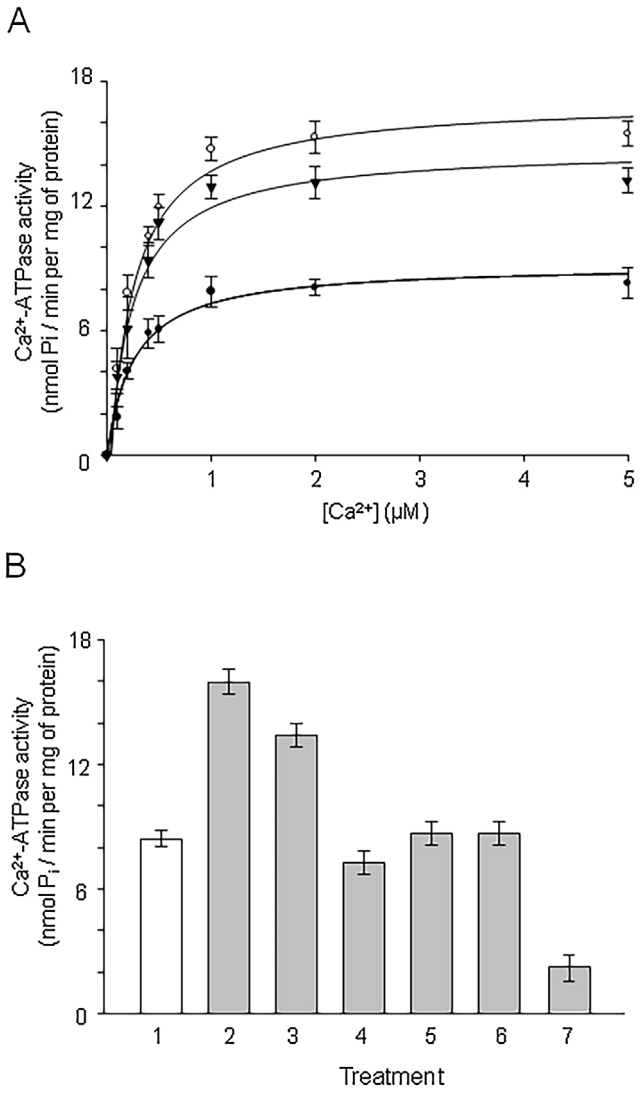

Fig. 2. Ca^{2+}-ATPase activity in plasma membrane fraction from *T. equiperdum.* A) Activation by calmodulin. Ca^{2+}-ATPase activity in the presence of: (▼) bovine CaM (8 μg/ml), (○) *T. cruzi* CaM (8 μg/ml) and (●) without CaM, basal activity. B) Evaluation of different modulators and inhibitor at Ca^{2+} saturate concentration (10 μM). (1) Basal Ca^{2+}-ATPase activity, (2) *T. cruzi* CaM (8 μg/ml), (3) bovine CaM (8 μg/ml), (4) CMZ (10 μM), (5) CMZ (10 μM) + *T. cruzi* CaM (8 μg/ml), (6) Oligomycin (1 μg/ml) and (7) Vanadate (20 μM). The values represent the mean ± SD for at least six determinations for each condition.

[15,24]. As shown in Fig. 2B, when vanadate (20 μM) was added to the medium, a significant inhibition of the Ca^{2+}-ATPase activity was detected (2.1 ± 0.65 nmol Pi/min per mg protein), corresponding to 75% inhibition of basal activity. Additionally, Ca^{2+}-ATPase activity was not significantly inhibited by classical mitochondrial ATPase inhibitor such as oligomycin (8.66 ± 0.53 nmol Pi/min per mg protein, $P < 0.05$) indicating that the preparation used was not contaminated by mitochondrial membrane (Fig. 2B).

3.3. Evaluation of the interaction between CaM and the plasma membrane Ca^{2+}-ATPase from T. equiperdum

The direct interaction between CaM and TePMCA was evaluated employing biotinylated-CaM labeling in the presence and absence of Ca^{2+}. Fig. 3A shows the labeling of purified human erythrocytes PMCA (140 kDa, Fig. 3A strip Hs) and a band of about 120 kDa (Fig. 3A strip Te) representing the PMCA of *T. equiperdum* in the TePMF, in the presence of Ca^{2+}. This labeled protein has a similar

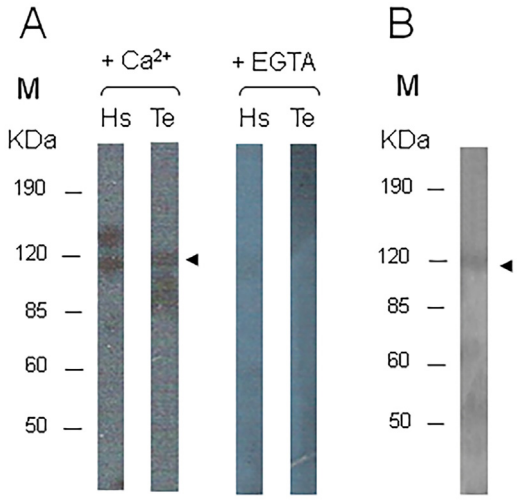

Fig. 3. Evaluation of the binding of calmodulin with the PMCA. A) Labeling of PMCA with biotinylated calmodulin. Lanes Hs: purified PMCA from human erythrocyte; lanes Te: plasma-membrane fraction from *T. equiperdum*. Incubations with biotinylated CaM were performed in presence and absence of Ca^{2+}, with EGTA (0.2 mM $CaCl_2$ or 1 mM EGTA). B) Purification of PMCA form *T. equiperdum* by affinity chromatography. Silver-stained SDS-PAGE of the fraction CaM-sepharose column eluent in absence of Ca^{2+}, with EDTA (2 mM). M: molecular weight marker. Arrow indicates the 120 molecular mass bands corresponding to *T. equiperdum* PMCA.

molecular weight to that recognized by PMCAs specific antibodies. Additionally, some derived proteolytic fragments of lower molecular mass are also apparent in both cases. Instead, in the absence of Ca^{2+} no labeling was observed, indicating that the interaction between these two proteins is Ca^{2+}-dependent.

This interaction was further supported by the TePMCA purification using a CaM-sepharose affinity column. Fig. 3B shows a SDS-PAGE of the eluted fraction from a CaM-sepharose column after removing Ca^{2+} from the medium. It can be observed a band of molecular mass slightly less than 120 kDa, corresponding to the expected for TePMCA, and consistent with the result of biotinylated-CaM labeling. This methodology has been conventionally used for the purification of PMCAs from higher eukaryotic [57] and trypanosomatids [17]. Thus, the above results support the presence of a CaM-BD in the TePMCA.

3.4. Cloning and identification of PMCA characteristic domains in the sequence of the putative plasma membrane Ca^{2+}-ATPase from T. equiperdum

A sequence of 3543 bp belonging to the putative TePMCA gene was cloned by PCR using the parasite genomic DNA. This gene codes for a protein of 1080 amino acids, with an estimated molecular mass of 118.9 kDa and a theoretical isoelectric point (pI) of 6.47, similar to other described PMCAs from higher eukaryotes and other trypanosomatids. The genomic sequence of the putative TePMCA gene was deposited in the GenBank under the submission ID KY073239. The deduced amino acid sequence has 31% similarity with human PMCA4b. Despite the low homology between the human PMCA4b and TePMCA sequences, functional domains are highly conserved (Fig. 4).

Structurally, the TePMCA is similar to their higher eukaryotes counterparts. Alignment between human PMCA4b and TePMCA (Fig. 4A) revealed that the TePMCA protein contains all the invariant residues and conserved motifs found in other P-type ATPases. Thus, the classical phosphorylation sequence holding the critical D residue, the ATP binding domain containing the K residue, the actuator domain and the Ca^{2+} translocation sites are present in TePMCA. Hydrophobicity analysis of the sequence (data not shown) revealed

Table 2
Calmodulin binding motifs provide by Calmodulation Database and Meta-Analysis prediction server in *T. equiperdum* PMCA C-terminal region.

Motif	Sequence	Residues
1–10	LRAQSRWRRL	1033–1042
	VKKPRVVNAF	1047–1056
1–12	LLAGRLRAQSRW	1028–1039
	LQAEHVKKPRVV	1042–1053
1–14	LAGRLRAQSRWRRL	1029–1042
	WRRLQAEHVKKPRV	1039–1052
	VKKPRVVNAFRRAW	1047–1060
	WTDRDMKRGSTRQL	1060–1073

that TePMCA possesses 10 potential transmembrane domains and three cytoplasmic regions, where the C-terminal domain extends from the last transmembrane domain to the end of the protein, similar to other Ca^{2+} pumps [6,7]. Fig. 4A also shows the sequence in PMCA4b recognized by antibody 5F10. A similar region for this antibody was observed in TePMCA, where 11 residues are identical and there are only 4 non conservative substitutions. The deduced amino acid sequence has 63%, 56% and 99% homology with *T. cruzi* [19], *L. major* [58], and *T. brucei* [20], respectively; and shares 31% identity with PMCA4b from *Homo sapiens* [46].

Interestingly, the analysis of the C-terminal region from TePMCA (1001–1080 residues) by the Calmodulation Database and Meta-Analysis Predictor (CDMAP) server (http://cam.umassmed.edu) [49], predicts a potential CaM-BD of 33 residues based on the density of canonical binding motifs (Fig. 4B) This server searches for the presence of bulky hydrophobic residues F, I, L, V, W, and Y, at the first and last position of the binding region in the sequence target, which provide the anchors for the peptide into the two CaM lobes [49]. As shown in Table 2, the program predicted a number of patterns resembling the canonical classical 1–10, 1–12, 1–14 Ca^{2+}/CaM-binding motifs, and did not detected the classical 1–8-14, 1–5-8-14, 1–16, or IQ motifs in the C-terminal region from TePMCA. The 1–14 motif described for the PMCA4b is included within the potential CaM-BD predicted, which has the W and V anchors residues [12,13,59]. However, biochemical evidences (synthetic peptide and mutagenesis) have shown that the presence of the amino acids W_{1093} and F_{1110} in the C28 peptide is necessary to achieve the maximum inhibition of PMCA4b stimulation by CaM [60,61]. These results suggested that the CaM-binding motif classification of the PMCA4b is 1–18, with these aromatic amino acids as anchors [62].

Although the CDMAP server does not search for 1–18 motifs, the alignment of our sequence with the C-terminal of PMCA regions from species with different evolutionary levels, all described as CaM-sensitive by biochemical studies [15,17,25,62,63], allowed us to define the TeC28 peptide within the CaM-BD predicted (S_{1027}-W_{1060}), which contains non-classical 1–18 motif (Fig. 4B). Additionally, this region presents a sequence which has an identity of 28.57% with the C28 peptide described in PMCA4b as CaM-BD (Fig. 4B), in which the anchor amino acids W and F are conserved, characteristic of a 1–18 motif described by Juranic et al. [14].

In general, a defined consensus sequence for a CaM-binding site does not exist and does not share high sequence similarity [64]. Moreover, the remaining intermediate residues between the anchors are highly variable in the sequence and spacing because the helix connecting the CaM lobes acts as a flexible hinge [65,66], enabling CaM to bind between hydrophobic anchor residues with a broad range of spacing residues. It is possible that due to the large structural flexibility of CaM, this protein could bind to a wide range of potentially CaM binding motifs identified in the TePMCA C-terminal domain. The canonical motifs, such as the 1–10 and1-12, that are present in C-terminal from TePMCA (Table 2) have

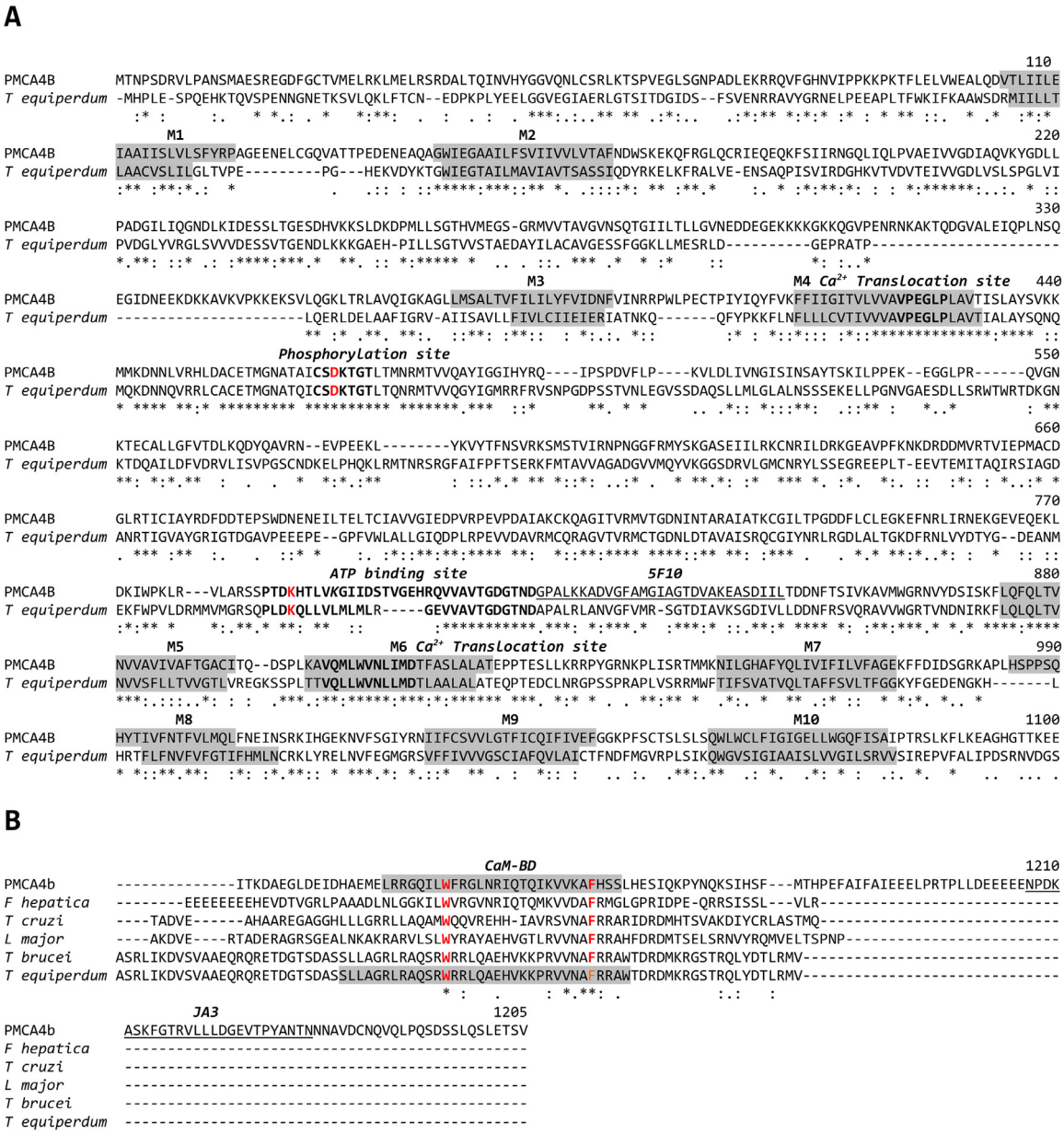

Fig. 4. Putative Ca^{2+}-ATPase amino acid sequence from *T. equiperdum*.
A) Clustal Omega alignment of *T. equiperdum* PMCA (GI KY073239) and Homo sapiens PMCA4b (GI 48255957). Identical residues are shown with an asterisk (∗), conservative substitutions are labeled with a colon (:), and semi-conservative substitutions are labeled with a period (.). Transmembrane segments M1–M10 are shaded in grey. The phosphorylation, ATP binding, and Ca^{2+} translocation site are highlighted in bold, indicating D and K residues in red bold. Antibody epitope for 5F10 is underline. B) Alignment of various PMCA C-terminal regions. Clustal Omega multiple alignment of *T. equiperdum* (1001–1080 residues, GenBank access number 1899016), *T. brucei* (GI 72392312), *Leishmania* sp. (GI 157864519), *T. cruzi* (GI 2992501), *F. hepatica* (GI 392856267) and *Homo sapiens* PMCA4b (GI 48255957). The CaM-binding domain (CaM-BD) prediction by the Calmodulation Database and Meta-Analysis Predictor server in *T. equiperdum* and C28 of the PMCA4b are shaded in grey and anchors residues for 1–18 motif are highlight in red bold. Antibody epitope for JA3 in PMCA4b is underline.

been described in other CaM-modulated proteins such as CaM-dependent protein-kinase II, MLCK and KCNQ channels [49,64,67].

Additionally, Fig. 4B shows another difference between TePMCA and PMCA from higher eukaryotes, it is a shorter C-terminal domain, lacking the sequence recognized by the JA3 antibody. This information explains the results obtained with the immunostaining described above in Fig. 1A.

3.5. *Modeling and structural features of the PMCA from* T. equiperdum

The general architecture of the pump, as deduced by a variety of secondary structure programs, shows that most of 80% of the topological model proposed for the TePMCA is exposed to the cytosolic side (Fig. 5A), similar to counterparts described for higher eukaryotic [6,7]. Three cytoplasmic regions and 10 transmembrane domains (1–10) of the enzyme can be observed. The first cytoplasmic region encloses the "actuator domain" (A), which gaiting mechanism regulates Ca^{2+} binding and release and the second, being the largest, located between M4 and M5 transmembrane regions, contains the phosphorylation (P) and the ATP binding (N) domains. The third protruding domain following the tenth transmembrane helix presents a putative CaM-BD localized at the C-terminal tail (Fig. 5A).

Despite some differences in amino acid sequence, our results suggest that TePMCA folds in a similar manner to "P-type" Ca^{2+}-

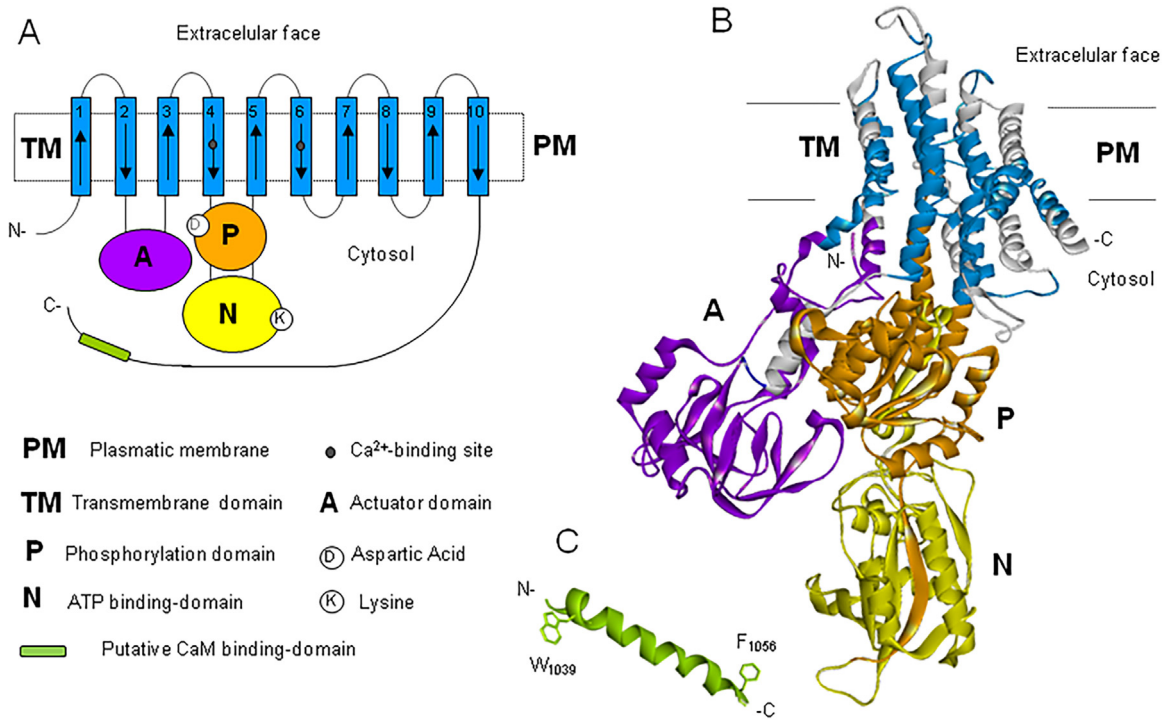

Fig. 5. *Trypanosoma equiperdum* PMCA model. A) Topologic model. B) Predicted structure of the TePMCA (residues 1–982) positioned such that the four key domains are visible. The transmembrane domains (TM) (Blue) are at the top, with the actuator (A) (purple), phosphorylation (P) (orange) and nucleotide-binding (N) (yellow) domains. C) Putative CaM binding domain (green). (For interpretation of the references to colour in this figure legend, the reader is referred to the web version of this article.).

ATPase proteins from higher eukaryotes. Fig. 5B shows a predicted three-dimensional structure of the TePMCA obtained by employing the Phyre2 web portal for protein modeling, prediction and analysis server [50]. TePMCA homology modeling identified a rabbit SERCA1 protein (PDB: c3b9bA) as the most appropriate template in the absence of any experimentally determined PMCA structures [49], where 914 residues (85% of the sequence) were modeled with 100% confidence using this highest template. The predicted structure shows the same domains described in the topologic model, except for the CaM-BD (Fig. 5B). The estimated value for the root mean square deviation (RMSD) was 1.83 Å for the Cα atoms suggesting a slight deviation of our model from the reference crystal structure. Examination of the Ramachandran plot indicated a good overall geometry for the TePMCA (phi/psi 85.6%). As expected, the tertiary structure of these proteins is more conserved than their primary structure (Fig. 6A).

The C-terminal modeling of TePMCA by Phyre2 (985–1080 residues) predicted a helical region, localized between amino acids $\mathbf{R}_{1026}$–$\mathbf{R}_{1058}$ using the chain B of PDB structure 2kne, as the most appropriate template (Fig. 5C). The chain B (C28 peptide) corresponds to the CaM-BD from human PMCA4b recently confirmed in the NMR structure study [14]. This region consists of 28 residues from TePMCA (TeC28), of which 24 adopts an α-helix, modeled with 74.2% confidence by the single highest scoring template. Therefore, the analysis by Phyre2 established that this peptide shares homology with the C28 from the 2kne structure. It is important

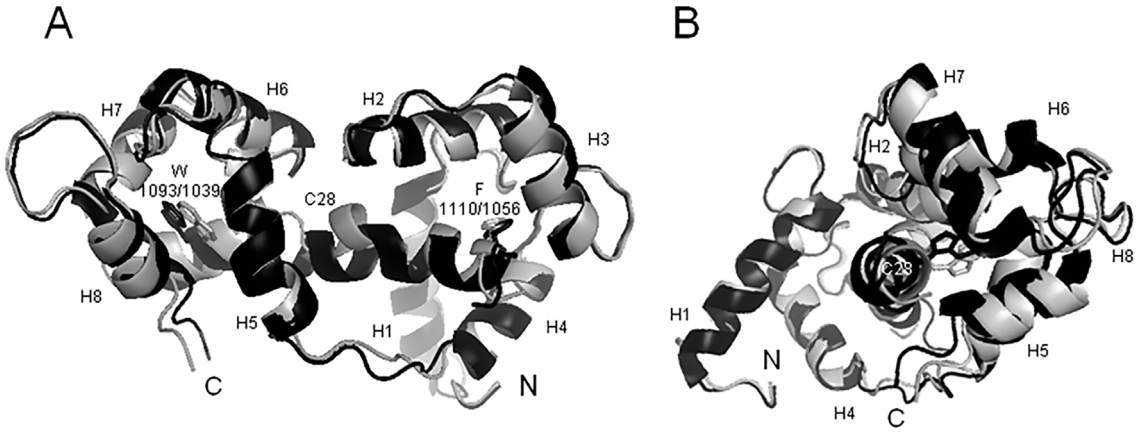

Fig. 6. Superposition of TcCaM-TeC28 docking with 2KNE complex. Structures in grey TcCaM-TeC28 and in black the PDB entry 2Kne. Viewed: A) along the bound peptide, side view and (B), rotated 90° with the N-terminus of the bound peptide on top, front view. The α-helices of the CaMs are labeled (H1-H8) and anchor residues ($F_{1110/1057}$ and $W_{1093/1039}$) are shown in lines.

to highlight that even though the low identity of TeC28 with the C28 from PMCA4b, the peptide presented all the necessary characteristic to be considered as a CaM-BD for TePMCA: a high helix propensity with a net positive charge (9 at pH 7.0), a moderate hydrophobicity, and two conserved hydrophobic amino acid anchors (W_{1039} and F_{1056}), spaced by 18 residues.

3.6. *Docking of* T. cruzi *CaM with* T. equiperdum *C28*

CaM is a highly conserved protein throughout evolution, with a 90% identity between *T. cruzi* and *Homo sapiens*. This level of conservation allows the homology modeling of TcCaM using chain A from 2kne [14] as a template in the reference structure. The TcCaM model obtained from the Swiss-Model server presented a RSMD value of 0.89 Å with respect to the A chain from reference structure (2kne). This conserved identity was reflected in the RSMD value < 1 Å obtained for TcCaM, indicating a high similarity between these structures. The TcCaM model and the sequence of the TeC28 peptide (TeCaM-BD) from the C-terminal region of TePMCA, were submitted to CABS-dock web server to obtain a molecular docking. The server performs simulation searches for the binding site allowing peptide flexibility and small fluctuations from the receptor backbone and provides an interface for modeling receptor-ligand interactions. From the final 10 models generated by the server, only the protein complex with the closest resemblance to the reference structure and the lowest RMSD, with a value of 1.20 Å, was selected. Fig. 5 shows the TcCaM-TeC28 docking complex, which readily superimposed to the reference structure. The TcCaM-TeC28 docking complex exhibited a binding orientation in an anti-parallel manner. The TeC28 peptide adopted an amphipathic helical conformation between the 2 anchor residues. The aromatic rings of the $W_{1093/1039}$ and $F_{1110/1056}$ anchors were buried inside the hydrophobic pockets of the CaM lobes. The structure revealed a typical CaM-binding mode, with both CaM-lobes wrapping around the target helical peptide (Fig. 5A and B). The estimated RSMD value for the ligand was 2.31 Å. Despite the low identity for TeC28, the ligand-RMSD is slightly more than 2 Å, indicating a high accuracy in agreement with the quality assessment criteria described by Blaszczyk et al. [69]. Therefore, the molecular docking of TcCaM-TeC28 complex shows a significant similarity with the reference structure (2kne) used for the docking protocol developed in this study.

Other parameters used to establish the possible interaction between TeC28 and TcCaM was the energy required for ligand and receptor interactions. The binding energy generated using Hex 8.0 program [54] for this structure was very low, with a value of −661 kj/mol. Lower values of negative energy indicate a tight ligand-receptor bond; on the contrary, high energy values may cause instability or binding difficulties between ligand and receptor. Therefore, the low value of binding energy obtained indicated that the interactions between the ligand (TeC28) and its receptor (TcCaM) were favorable, suggesting that there was a high probability of binding and a high stability for the overall structure.

The docking TcCaM-TeC28 complex was easily superimposed on the reference structure (2kne), sharing common characteristics for the canonical binding mechanism from Ca^{2+}/CaM-complexes determined by crystal structure and NMR [14,64,65]. The docking complexes exhibits a globular conformation, where the peptide adopts a predominant helical structure in the N- and C- terminal regions, with some distortion from ideal α-helix conformation in the middle, possibly due to the presence of a P residue in the sequence. Nevertheless, TcCaM wrapped around TeC28 peptide using the two hydrophobic anchor residues (W and F), which are buried in the hydrophobic pockets of CaM-lobes in an anti-parallel interaction, at positions 18 and 1, as in reference structure. Analysis of the geometry of Ca^{2+}/CaM binding peptides with these characteristics established that only relative sequential positions of 10, 14, 17, and 18, are allowed for the second anchor [14]. Likewise, the docking contact map provide by the server of the interface interaction between TcCaM with the residues $W_{1093/1040}$ and $F_{1110/1057}$, showing that the hydrophobic interactions are highly conserved in the pockets (data not show), similar to the described for 2kne [14,70]. It should be pointed out that the M and the aliphatic (L, I and V) residues are conserved, which play an important role in the CaM-binding to anchor amino acids, keeping the hydrophobic binding surface [64]. However, the presence of a long distance 1–18 CaM-binding motif in TeC28, can only be possible due to the high flexibility of CaM lobes rotation around the central linker and by the dynamic repositioning of side chain conserved residues that makes the hydrophobic pockets highly conformationally adaptable, rearranging the lobes to create an optimal interaction surface.

4. Conclusion

This study provides evidence that *T. equiperdum* possess a functional PMCA which shares biochemical and structural similarity with Ca^{2+} pumps from higher eukaryotes. Our experiments showed a Ca^{2+}/CaM sensitive PMCA and allow us to propose a 28 amino acid residue domain in the C-terminal tail as a non-canonical CaM binding domain within a 1–18 motif. Structural analysis of a CaM-peptide complex revealed diverse binding modes and a large conformational CaM flexibility. Therefore, bioinformatics advances facilitate the discovery of novel mechanism in CaM binding and regulation in PMCA trypanosomatids, whose sensibility to CaM has been determined experimentally. More research using synthetic peptides, structural analyses and computational programming should be done to study the dynamics of the interaction between CaM and its target in the trypanosomatids.

Acknowledgements

We thank Dr. Juan Carlos Martinez and Alexandra Clemente for critically reading and correcting this manuscript. This work was supported by a grant from S1-14019 CDCHT—UNESR. Caracas, Venezuela and Prometeo Program SENESCYT-ECUADOR.

References

[1] M. Desquesnes, Trypanosomes, Pathogenecity, Clinical Sings, Diagnosis and Characterisation of Livestock Trypanosome in Latin America. En: Livestock Trypanosomoses and Their Vectors in Latin America, CIRAD French Agricultural Research Centre for International Development. OIE World Organization for Animal Health, Paris, France, 2004, pp. 7–32 (Capitulos 1 y 2).
[2] M. Desquesnes, P. Holzmuller, D.H. Lai, A. Dargantes, Z.R. Lun, S. Jittaplapong, *Trypanosoma evansi* and surra: a review and perspectives on origin, history, distribution, taxonomy, morphology, hosts, and pathogenic effects, BioMed Res. Int. (2013) http://dx. 10.1155/2013/194176.
[3] G. Benaim, C.R. García, Targeting calcium homeostasis as the therapy of Chagas' disease and leishmaniasis—a review, Trop. Biomed. 28 (2011) 471–481.
[4] M.R. Duchen, Mitochondria and calcium: from cell signalling to cell death, J. Physiol. 15 (Pt. (1)) (2000) 57–68, 529.
[5] B. Zhivotovsky, S. Orrenius, Calcium and cell death mechanisms: a perspective from the cell death community, Cell Calcium 50 (2011) 211–221 http://dx.10.1016/j.ceca.2011.03.003.
[6] M. Brini, E. Carafoli, Calcium pumps in health and disease, Physiol. Rev. 89 (2009) 1341–1378 http://dx.10.1152/physrev.00032.2008.
[7] M. Brini, E. Carafoli, The plasma membrane Ca^{2+} ATPase and the plasma membrane sodium calcium exchanger cooperate in the regulation of cell calcium, Cold Spring Harb Perspect. Biol. 1 (3 (2)) (2011) http://dx.10.1101/cshperspect.a004168.
[8] M. Brini, T. Calì, D. Ottolini, E. Carafoli, Intracellular calcium homeostasis and signaling, Met. Ions Life Sci. 12 (2013) 119–168 http://dx.10.1007/978-94-007-5561-1_5.
[9] G. Benaim, M. Zurini, E. Carafoli, Different conformational states of purified Ca^{2+}-ATPase of the erythrocyte plasma membrane revealed by controlled trypsin proteolysis, J. Biol. Chem. 259 (1984) 8471–8477.

[10] R. Falchetto, T. Vorherr, E. Carafoli, The calmodulin-binding site of the plasma membrane Ca^{2+} pump interacts with the transduction domain of the enzyme, Protein Sci. 1 (1992) 1613–1621.
[11] A.K. Verma, A. Enyedi, A.G. Filoteo, J.T. Penniston, Regulatory region of plasma membrane Ca^{2+} pump. 28 residues suffice to bind calmodulin but more are needed for full auto-inhibition of the activity, J. Biol. Chem. 269 (1994) 1687–1691.
[12] A.R. Rhoads, F. Friedberg, Sequence motifs for calmodulin recognition, FASEB J. 11 (1997) 331–340.
[13] K.P. Hoeflich, M. Ikura, Calmodulin in action: diversity in target recognition and activation mechanisms, Cell 6 (2002) 739–742.
[14] N. Juranic, E. Atanasova, A.G. Filoteo, S. Macura, F.G. Prendergast, J.T. Penniston, E.E. Strehler, Calmodulin wraps around its binding domain in the plasma membrane Ca^{2+} pump anchored by a novel 18-1 motif, J. Biol. Chem. 6 (2010) 4015–4024 http://dx.10.1074/jbc.M109.060491.
[15] G. Benaim, C. Lopez-Estraño, R. Docampo, S.N. Moreno, A calmodulin-stimulated Ca^{2+} pump in plasma-membrane vesicles from *Trypanosoma brucei*; selective inhibition by pentamidine, Biochem. J. 296 (1993) 759–763.
[16] S.N. Moreno, R. Docampo, Calcium regulation in protozoan parasites, Curr. Opin. Microbiol. 6 (2003) 359–364.
[17] G. Benaim, S.N. Moreno, G. Hutchinson, V. Cervino, T. Hermoso, P.J. Romero, F. Ruiz, W. de Souza, R. Docampo, Characterization of the plasma-membrane calcium pump from *Trypanosoma cruzi*, Biochem. J. 306 (1995) 299–303.
[18] S. Mazumder, T. Mukherjee, J. Ghosh, M. Ray, A. Bhaduri, Allosteric modulation of *Leishmania donovani* plasma membrane $Ca^{(2+)}$-ATPase by endogenous calmodulin, J. Biol. Chem. 267 (1992) 18440–18446.
[19] H.G. Lu, L. Zhong, W. de Souza, M. Benchimol, S. Moreno, R. Docampo, Ca^{2+} content and expression of an acidocalcisomal calcium pump are elevated in intracellular forms of *Trypanosoma cruzi*, Mol. Cell. Biol. 18 (1998) 2309–2323.
[20] S. Luo, P. Rohloff, J. Cox, S.A. Uyemura, R. Docampo, *Trypanosoma brucei* plasma membrane-type $Ca^{(2+)}$-ATPase 1 (TbPM) and 2 (TbPMC2) genes encode functional $Ca^{(2+)}$-ATPases localized to the acidocalcisomes and plasma membrane, and essential for $Ca^{(2+)}$ homeostasis and growth, J. Biol. Chem. 279 (2004) 14427–14439 http://dx.10.1074/jbc.M309978200.
[21] R. Docampo, G. Huang, Calcium signaling in trypanosomatid parasites, Cell Calcium 57 (2015) 194–202, http://dx.doi.org/10.1016/j.ceca.2014.10.015.
[22] G. Benaim, S. Losada, F.R. Gadelha, R. Docampo, A calmodulin-activated $(Ca^{2+}$-$Mg^{2+})$-ATPase is involved in calcium transport by plasma membrane vesicles from Trypanosoma cruzi, Biochem. J. 280 (1991) 715–720.
[23] M.A. Cataldi de Flombaum, A.O. Stoppani, High-affinity calcium-stimulated, magnesium-dependent adenosine triphosphatase in *Trypanosoma cruzi*, Comp. Biochem. Physiol. B 103 (1992) 933–937.
[24] G. Benaim, P.J. Romero, A calcium pump in plasma membrane vesicles from *Leishmania braziliensis*, Biochim. Biophys. Acta 1027 (1990) 79–84.
[25] G. Benaim, V. Cervino, T. Hermoso, P. Felibert, A. Laurentin, Intracellular calcium homeostasis in *Leishmania mexicana*. Identification and characterization of a plasma membrane calmodulin-dependent $Ca^{(2+)}$-ATPase, Biol. Res. 26 (1993) 141–150.
[26] R. Brun, H. Hecker, Z.R. Lun, *Trypanosoma evansi* and *T. equiperdum*: distribution biology, treatment and phylogenetic relationship (a review), Vet. Parasitol. 79 (1998) 95–107.
[27] V. Prasad, G.W. Okunade, M.L. Miller, G.E. Shull, Phenotypes of SERCA and PMCA knockout mice, Biochem. Biophys. Res. Commun. 322 (2004) 1192–1203 http://dx.10.1016/j.bbrc.2004.07.156.
[28] T.M. Dinamarco, F.Z. Freitas, R.S. Almeida, N.A. Brown, T.F. dos Reis, L.N. Ramalho, M. Savoldi, M.H. Goldman, M.C. Bertolini, G.H. Goldman, Functional characterization of an Aspergillus fumigatus calcium transporter (PmcA) that is essential for fungal infection, PLoS One 7 (5) (2012) e37591 http://dx.10.1371/journal.pone.0037591.
[29] T.M. Perrone, M.I. Gonzatti, G. Villamizar, A. Escalante, P.M. Aso, Molecular profiles of Venezuelan isolates of *Trypanosoma* sp. by random amplified polymorphic DNA method, Vet. Parasitol. 161 (2009) 194–200 http://dx.10.1016/j.vetpar.2009.01.034.
[30] S.M. Lanham, D.G. Godfrey, Isolation of salivarian Trypanosome from man and other mammals using DEAE Cellulose, Exp. Parasiol. 28 (1970) 521–534.
[31] E. Espinoza, N. González, G. Primera, M. Desquesnes, L. Hidalgo, Sobrevivencia del Trypanosoma vivax (cepa I IV) y Trypanosoma evansi (cepaTEVAl) en condiciones experimentales, Trop. Vet. 22 (1997) 189–194.
[32] M. Mendoza, A. Mijares, H. Rojas, C. Colina, V. Cervino, R. DiPolo, G. Benaim, Evaluation of the presence of a thapsigargin sensitive calcium store in *Trypanosoma evansi* as a model, J. Parasitol. 90 (2004) 1181–1183 http://dx.10.1645/GE-263R.
[33] M.C. Pérez-Gordones, M.L. Serrano, H. Rojas, J.C. Martínez, G. Uzcanga, M. Mendoza, Presence of a thapsigargin-sensitive calcium pump in *Trypanosoma evansi*: immunological, physiological, molecular and structural evidences, Exp. Parasitol. 159 (2015) 107–117 http://dx.10.1016/j.exppara.2015.08.017.
[34] E. Sánchez, T.M. Perrone, G. Recchimuzzi, I. Cardozo, N. Biteau, A. Mijares, T. Baltz, D. Berthier, L. Balzano-Nogueira, M.I. Gonzatti, P.M. Aso, Molecularcharacterization and classification of *Trypanosoma* spp. Venezuelan isolatesbased on microsatellite markers and kinetoplast maxicircle genes, Parasites Vectors 8 (2015) 536–547 http://dx.10.1186/s13071-015-1129-2.
[35] O.H. Lowry, N.J. Rosebrough, A.L. Farr, R.J. Randall, Protein measurement with the folin phenol reagent, J. Biol. Chem. 193 (1951) 265–275.
[36] C.H. Fiske, Y. Subbarow, The colorimetric determination of phosphorus, J. Biol. Chem. 66 (1925) 375–400.
[37] A. Fabiato, F. Fabiato, Calculator programs for computing the composition of the solutions containing multiple metals and ligands used for experiments in skinned muscle cells, J. Physiol. 75 (1979) 463–505.
[38] Y. Garcia-Marchan, F. Sojo, E. Rodriguez, N. Zerpa, C. Malave, I. Galindo-Castro, M. Salerno, G. Benaim, *Trypanosoma cruzi* calmodulin: cloning, expression and characterization, Exp. Parasitol. 123 (2009) 326–333 http://dx.10.1016/j.exppara.2009.08.010.
[39] U.K. Laemmli, Cleavage of structural proteins during the assembly of the head of bacteriophage T4, Nature 227 (1970) 680–685.
[40] H. Towbin, T. Staehelin, J. Gordon, Electrophoretic transfer of proteins from polyacrylamide gels to nitrocellulose sheets: procedure and some applications, Proc. Natl. Acad. Sci. U. S. A. 76 (1979) 4350–4354.
[41] B.T. Kurien, Affinity purification of autoantibodies from an antigen strip excised from a nitrocellulose protein blot, Methods Mol. Biol. 536 (2009) 201–211.
[42] M.L. Billingsley, K.R. Pennypacker, C.G. Hoover, D.J. Brigati, R.L. Kincaid, A rapid and sensitive method for detection and quantification of calcineurin and calmodulin-binding proteins using biotinylated calmodulin, Proc. Natl. Acad. Sci. U. S. A. 82 (1985) 7585–7589.
[43] F. Sanger, S. Nicklen, A.R. Coulson, DNA sequencing with chain-terminating inhibitors, Proc. Natl. Acad. Sci. U. S. A. 74 (1977) 5463–5467.
[44] C. Combet, C. Blanchet, C. Geourjon, G. Deléage, NPS@: network protein sequence analysis, Trends Biochem. Sci. 25 (2000) 147–150.
[46] P. James, M. Maeda, R. Fischer, A.K. Verma, J. Krebs, J.T. Penniston, E. Carafoli, Identification and primary structure of a calmodulin binding domain of the Ca^{2+} pump of human erythrocytes, J. Biol. Chem. 263 (1988) 2905–2910.
[47] G. von Heijne, Membrane protein structure prediction: hydrophobicity analysis and the positive-inside rule, J. Mol. Biol. 225 (1992) 487–494.
[48] G.E. Tusnády, I. Simon, The HMMTOP transmembrane topology prediction server, Bioinformatics 17 (2001) 849–850.
[49] K. Mruk, B.M. Farley, A.W. Ritacco, W.R. Kobertz, Calmodulation meta-analysis: predicting calmodulin binding via canonical motif clustering, J. Gen. Physiol. 144 (2014) 105–114 http://dx.10.1085/jgp.201311140.
[50] C. Olesen, M. Picard, A.M. Winther, C. Gyrup, J.P. Morth, C. Oxvig, J.V. Møller, P. Nissen, The structural basis of calcium transport by the calcium pump, Nature 450 (2007) 1036–1042 http://dx.10.1038/nature06418.
[51] L.A. Kelley, S. Mezulis, C.M. Yates, M.N. Wass, M.J. Sternberg, The Phyre2 web portal for protein modeling, prediction and analysis, Nat. Protoc. 10 (2015) 845–858 http://dx.10.1038/nprot.2015.053.
[52] R.A. Laskowski, M.W. MacArthur, D.S. Moss, J.M. Thornton, PROCHECK: a program to check the stereochemical quality of protein structures, J Appl. Cryst. 26 (1993) 283–291, http://dx.doi.org/10.1107/S0021889892009944.
[53] M. Kurcinski, M. Jamroz, M. Blaszczyk, A. Kolinski, S. Kmiecik, CABS-dock web server for the flexible docking of peptides to proteins without prior knowledge of the binding site, Nucleic Acids Res. 1 (43 (W1)) (2015) W419–W424 http://dx.10.1093/nar/gkv456.
[54] G. Macindoe, L. Mavridis, V. Venkatraman, M.D. Devignes, D.W. Ritchie, HexServer: an FFT-based protein docking server powered by graphics processors, Nucleic Acids Res. 38 (2010) W445–W449 (Web Server issue) http://dx.10.1093/nar/gkq311.
[55] J.L. Borke, A. Caride, A.K. Verma, J.T. Penniston, R. Kumar, Plasma membrane calcium pump and 28-kDa calcium binding protein in cells of rat kidney distal tubules, Am. J. Physiol. 257 (1989) F842–F849.
[56] A.E. Vercesi, D.V. Macedo, S.A. Lima, F.R. Gadelha, R. Docampo, Ca^{2+} transport in digitonin-permeabilized trypanosomatids, Mol. Biochem. Parasitol. 42 (1990) 119–124.
[57] V. Niggli, E. Carafoli, The plasma membrane $Ca^{(2+)}$ ATPase: purification by calmodulin affinity chromatography, and reconstitution of the purified protein, Methods Mol. Biol. 1377 (2016) 57–70 http://dx.10.1007/978-1-4939-3179-8_7.
[58] A.C. Ivens, C.S. Peacock, E.A. Worthey, L. Murphy, G. Aggarwal, M. Berriman, The genome of the kinetoplastid parasite, *Leishmania major*, Science 309 (2005) 436–442 http://dx.10.1126/science.1112680.
[59] A.R. Penheiter, A.J. Caride, A. Enyedi, J.T. Penniston, Tryptophan 1093 is largely responsible for the slow off rate of calmodulin from plasma membrane Ca^{2+} pump 4b, J. Biol. Chem. 277 (2002) 17728–17732 http://dx.10.1074/jbc.M111608200.
[60] A. Enyedi, T. Vorherr, P. James, D.J. McCormick, A.G. Filoteo, E. Carafoli, J.T. Penniston, The calmodulin binding domain of the plasma membrane Ca^{2+} pump interacts both with calmodulin and with another part of the pump, J. Biol. Chem. 26421 (1989) 12313–12321.
[61] T. Vorherr, P. James, J. Krebs, A. Enyedi, D.J. McCormick, J.T. Penniston, E. Carafoli, Interaction of calmodulin with the calmodulin binding domain of the plasma membrane Ca^{2+} pump, Biochemistry 29 (1990) 355–365.
[62] A.R. Penheiter, A.G. Filoteo, J.T. Penniston, A.J. Caride, Kinetic Analysis of the calmodulin-binding region of the plasma membrane calcium pump isoform 4b, Biochemistry 44 (2005) 2009–2020 http://dx.10.1021/bi0488552.
[63] V. Niggli, E.S. Adunyah, J.T. Penniston, E. Carafoli, Purified $(Ca^{2+}$-$Mg^{2+})$-ATPase of the erythrocyte membrane: reconstitution and effect of calmodulin and phospholipids, J. Biol. Chem. 256 (1981) 395–401.
[64] C.M. Moore, E.M. Hoey, A. Trudgett, D.J. Timson, A plasma membrane $Ca^{(2+)}$-ATPase (PMCA) from the liver fluke, *Fasciola hepatica*, Int. J. Parasitol. 42 (2012) 851–858 http://dx. 10.1016/j.ijpara.2012.06.003.
[65] H. Tidow, P. Nissen, Structural diversity of calmodulin binding to its target sites, FEBS J. 280 (2013) 5551–5565 http://dx.10.1111/febs.12296.

[66] M. Ikura, S. Spera, G. Barbato, L.E. Kay, M. Krinks, A. Bax, Secondary structure and sidechain 1H and 13C resonance assignments of calmodulin in solution by heteronuclear multidimensional NMR spectroscopy, Biochemistry 30 (1991) 9216–9228.
[67] G. Barbato, M. Ikura, L.E. Kay, R.W. Pastor, A. Bax, Backbone dynamics of calmodulin studied by 15N relaxation using inverse detected two dimensional NMR spectroscopy: the central helix is flexible, Biochemistry 31 (1992) 5269–5278.
[69] M. Blaszczyk, M. Kurcinski, M. Kouza, L. Wieteska, A. Debinski, A. Kolinski, S. Kmiecik, Modeling of protein-peptide interactions using the CABS-dock web server for binding site search and flexible docking, Methods 93 (2016) 72–83 http://dx.10.1016/j.ymeth.2015.07.004.
[70] J.T. Penniston, A.J. Caride, E.E. Strehler, Alternative pathways for association and dissociation of the calmodulin-binding domain of plasma membrane Ca($^{2+}$)-ATPase isoform 4b (PMCA4b), J. Biol. Chem. 287 (2012) 29664–29671 http://dx.10.1074/jbc.M112.377556.